Mendeleev Communications

Mendeleev Commun., 2025, **35**, 586–588

End-group analysis to characterize the ring-opening polymerization of propylene oxalate

Nikolai P. Iakimov,[a] Ekaterina M. Budynina,[a,b] Evgenii O. Fomin,[a] Alexandra A. Egorova,[a] Anna K. Berkovich,[a] Marina V. Serebriakova,[c] Irina D. Grozdova[a] and Nikolay S. Melik-Nubarov*[a]

[a] *Department of Chemistry, M. V. Lomonosov Moscow State University, 119991 Moscow, Russian Federation. E-mail: melik.nubarov@belozersky.msu.ru*
[b] *P. N. Lebedev Physical Institute, Russian Academy of Sciences, 119991 Moscow, Russian Federation*
[c] *A. N. Belozersky Research Institute of Physico-Chemical Biology, M. V. Lomonosov Moscow State University, 119991 Moscow, Russian Federation*

DOI: 10.71267/mencom.7725

To get insight into attributes of propylene oxalate ring-opening polymerization catalyzed by $Sn(Oct)_2$, the polymerization was initiated by benzyl alcohol. According to ^{1}H NMR and MALDI-TOF mass spectrometry, the polymer chains were terminated by propylene glycol and benzyl residues, which amount correlated perfectly. The quantitative incorporation of the initiator into polyoxalates is the key to their functionalization and the synthesis of block-copolymers.

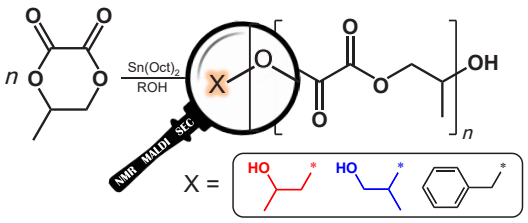

Keywords: propylene oxalate, ring-opening polymerization, polyoxalates, end-group analysis, transesterification.

Ring-opening polymerization (ROP), together with polycondensation, is a powerful tool for preparation of polyesters. In most cases, they are characterized by a considerable sustainability and biodegradability.[1] These polymers are of great interest for the development of suture materials,[2] self-absorbable wound dressings,[3] and temporary endoprostheses.[4] Biodegradable polymers are superior for the development of drug carriers which can decompose completely after fulfilment of their mission.[5] Polyoxalates stand out among polyesters due to their enhanced degradation rate.[6,7] The methods for their synthesis are mainly represented by polycondensation, which does not provide molecular weight control and tuning of the polymer architecture. Therefore, we have previously proposed the poly(propylene oxalate) (PPOx) synthesis by ROP.[8] This approach often provides good control of the molecular weight distribution and can be used for synthesis of amphiphilic block-copolymers,[9–11] which are applicable for drug delivery.[12–14] The formation of linear macromolecules and cyclic oligomers (Scheme 1) were found in the case of ROP of cyclic propylene oxalate (PrOx) initiated by hydrolyzed monomer impurities.[8] The molecular mass of macromolecules gradually increased with conversion. However, a detailed description of the process could not be performed using size exclusion chromatography (SEC) due to overlap of the peaks of macromolecules and oligomers, preventing the determination of the number-average molecular mass (M_n).

This problem can be solved by the end-group analysis. Inspection in macromolecules produced by ROP gives an opportunity to follow controllability of polymerization,[15,16] to determine the nature of end groups,[17–20] and to estimate M_n. So, the point of this paper was to find the end groups of PPOx obtained *via* ROP using NMR and MALDI-TOF mass spectrometry.

According to Scheme 1, the PPOx chains should contain two structurally non-equivalent fragments of propylene glycol (Pg) end groups affording different signals in the ^{1}H NMR spectrum.

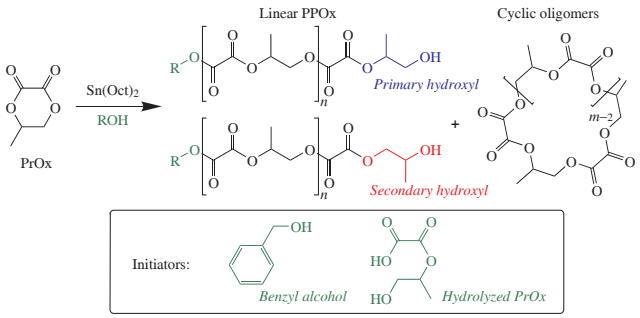

Scheme 1 Propylene oxalate ROP initiated by an alcohol (ROH, green) and catalyzed by $Sn(Oct)_2$. Terminal propylene glycol residues with free primary hydroxyl and, secondary hydroxyl are shown in blue and red, respectively. Indexes *n* and *m* denote the number of repeat units in the structures of linear and cyclic products, respectively.

In order to determine the ^{1}H NMR signals of these fragments, we synthesized a model oligo(propylene oxalate) with deliberately large quantity of hydroxyl end groups. To this end, PrOx reacted with the equimolar amount of Pg in the presence of tin(II) 2-ethylhexanoate [tin(II) octoate, $Sn(Oct)_2$] under inert conditions at 100 °C for 24 h. The reaction mixture was analysed by means of ^{1}H NMR spectroscopy (Figure S1). As discussed in Section S2 in Online Supplementary Materials, the two groups of peaks corresponding to primary and secondary OH groups were found (Figure S1).

The same set of signals as well as the signals of aromatic protons were detected in the ^{1}H NMR spectrum of the polymerization mixture obtained *via* ROP initiated by benzyl alcohol (BnOH) under equilibrium conditions (100 °C, 24 h) (Figure S2). The analysis of this sample by homonuclear correlation spectroscopy ^{1}H–^{1}H COSY (Figure S3) confirmed the assignment of the signals performed for the model system (Section S3 in Online Supplementary Materials).

The observed signals of hydroxyalkyl end groups were used to study the dependence of their content on the concentration of BnOH. It is convenient to follow the content of hydroxyl end groups by intensities of the peaks at 5.05 ppm (β-CH at primary hydroxyl, 1H) and at 4.06 ppm (α-CH and one of the β-CH_2 protons at secondary hydroxyl, 2H, see Figure S1). Increasing initiator concentration in the system enhanced both signals in parallel with the elevation of intensity of aromatic protons attributed to benzyl residues (7.3–7.4 ppm) [Figure 1(*a*)]. This clearly indicates that BnOH initiates ROP of PrOx, which leads to the hydroxyl end group formation according to Scheme 1. Both hydroxyl end group contents displayed a linear dependence on the initiator concentration, and the sum of their slopes was close to unity [Figure 1(*b*)]. It means that each BnOH molecule gave one hydroxyl end group (primary or secondary), indicating that the initiator was exhaustively consumed. Lines in Figure 1(*b*) deviate from the zero point due to the presence of the hydrolysed PrOx in the monomer sample.

Noteworthy, the concentration of secondary hydroxyl end groups in all samples was higher than that of primary ones. The ratio of the corresponding slopes in Figure 1(*b*) was 1.5 ± 0.1. This discrepancy can be attributed to either the selectivity of PrOx ring-opening, resulting predominantly in the formation of secondary hydroxyl end groups, or to the enhanced reactivity of primary hydroxyls in propagation or transesterification reactions (Section S4 in Online Supplementary Materials). The absence of regioregularity of PPOx found by ^{13}C NMR (X_{reg} ≈ 3%, Figure S4) indicates the nonselective character of PrOx ring-opening. Thus, the higher amount of the secondary hydroxyl end groups appears to be caused by their lower activity. This pattern is quite common for transesterification reactions between low-molecular-weight compounds.[21]

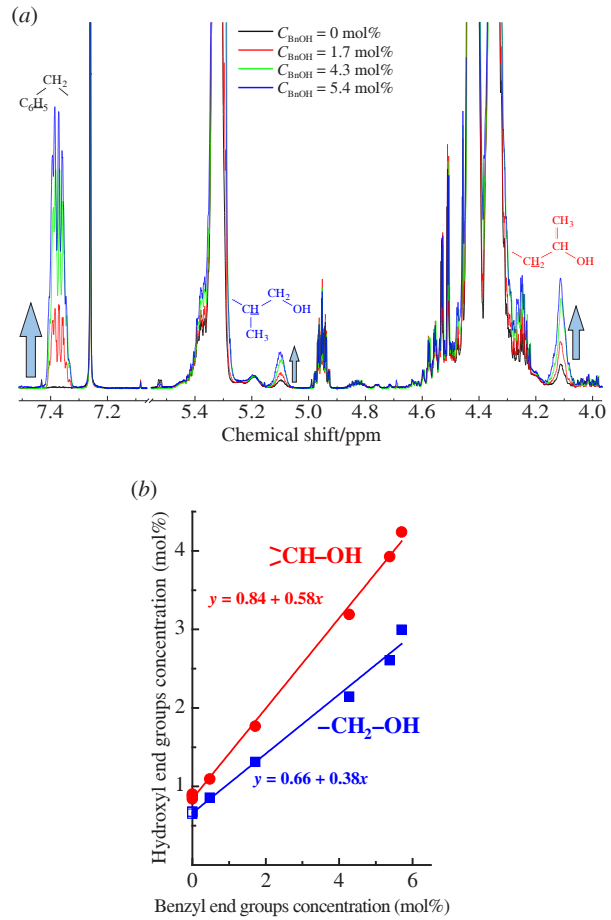

Figure 1 End-group analysis of the BnOH-initiated PPOx mixture by ^1H NMR. (*a*) ^1H NMR spectra of the samples obtained *via* PrOx polymerization catalysed by $Sn(Oct)_2$ (0.65 mol%) using different BnOH concentrations, 100 °C, 24 h. The structural fragments and arrows refer to the signals that were enhanced nearby. (*b*) BnOH concentration dependences of primary (blue) and secondary (red) hydroxyl end groups.

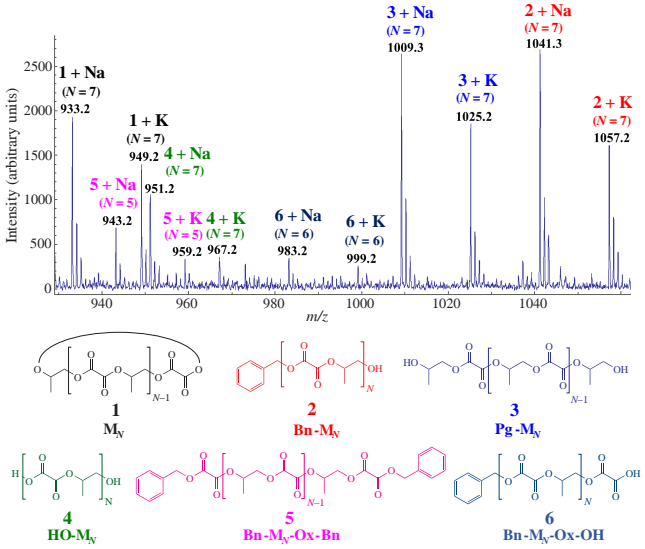

Figure 2 MALDI-TOF spectrum of the reaction mixture after PrOx polymerization for 24 h at 100 °C in the presence of 0.65 mol% of $Sn(Oct)_2$ and 8.8 mol% of BnOH. Structures revealed from the spectrum are shown beneath. Index *N* denotes the number of monomer repeat units (M) in the structures found by mass spectrometry.

A more detailed exploration of the types of end groups formed during PrOx polymerization was performed by means of MALDI-TOF mass spectrometry. The spectra of the reaction mixture after polymerization in the presence of BnOH showed six major groups of signals (Figure 2). Their *m/z* values grew up in steps of 130 corresponding to the PrOx molecular mass (Figure S7). Group **1** consists of the intense signals with masses divisible by 130 with the residues of 23 (Na^+) or 39 (K^+). The absence of any other residue means that group **1** corresponds to cyclic oligomers, in agreement with the previous data.[8]

The other five groups of signals correspond to linear macromolecules containing one of the three residues at each end, namely Pg, benzyl, or oxalate (Figure 2). The macromolecules grown from BnOH, Bn-M_N (Figure 2, type **2**), are the most abundant among the fractions with the linear structure. Comparable amounts of the polymer terminated with Pg fragments at both ends, Pg-M_N (Figure 2, type **3**) are observed. We also observed macromolecules started from the hydrolysed monomer, HO-M_N, (Figure 2, type **4**), as well as Bn-M_N-Ox-Bn (Figure 2, type **5**), and Bn-M_N-Ox-OH (Figure 2, type **6**), whose presence points to the intensive transesterification during ROP. The fraction of oxalate end groups in PPOx can be roughly estimated to be less than 10%.

Thus, MALDI-TOF examination confirmed that the terminal groups in PPOx were almost exclusively represented by benzyl and Pg residues. Their content estimated by ^1H NMR were used for calculation of the number-average polymerization degree P_n(NMR) according to the equation:

$$P_n(\text{NMR}) = \frac{2\omega C_{PrOx}}{C_{EG}}, \quad (1)$$

where C_{PrOx} is the concentration of PrOx consumed during polymerization, C_{EG} is the total concentration of end groups, and ω is the fraction of ROP linear products determined as described elsewhere.[8] Coefficient 2 reflects the existence of two end groups in PPOx.

SEC was used to check applicability of this equation. However, SEC analysis of PPOx obtained at high concentrations of the initiator [high C_{EG} in equation (1)] is complicated by the

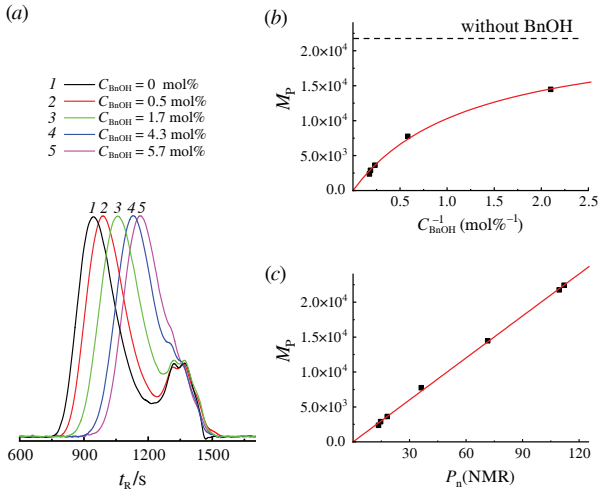

Figure 3 SEC analysis of ROP in the presence of various amounts of BnOH. (*a*) SEC traces of the reaction mixtures after ROP of PrOx (100 °C, 24 h) catalyzed by $Sn(Oct)_2$ (0.65 mol%) and initiated by BnOH (0–5.7 mol%). (*b*) Dependence of the peak mass (M_p) on C_{BnOH}^{-1}; and (*c*) dependence of M_p on P_n(NMR) calculated by equation (1).

overlap of the polymer peak with that of oligomers. Fractionation or subtracting of the oligomer peak significantly distorts the molecular weight distribution compared to the real one. Therefore, the peak mass M_p determined as abscissa of the maximum of SEC trace was used to estimate the changes in the molecular weight in such cases.[22]

An increase in the amount of BnOH added to the polymerization mixture gradually shifted the SEC pattern to lower molecular masses [Figure 3(*a*)]. The dependence of M_p on the reciprocal BnOH concentration, which should be linear theoretically, appeared to be hyperbolic and approached the plateau [Figure 3(*b*)]. This behavior is caused by the impurity of the hydrolyzed monomer involved in the ROP initiation.

The M_p values increased linearly with the growth of P_n(NMR) [Figure 3(*c*)], supporting the correctness of P_n determination from ^{1}H NMR spectra. Significantly, the dependence passes through the zero point, indicating the negligibly small amounts of end groups of unaccounted types. In contrast to the initiator, varying the catalyst content in the sample had virtually no effect on the polymer mass (Figure S8), which holds true for many systems.[23,24]

In conclusion, we discovered that the PPOx obtained by ROP contains almost exclusively propylene glycol and fragments of initiator (BnOH) as the end groups. The added initiator generates equivalent amounts of secondary and primary terminal Pg residues with a 1.5-fold excess of secondary ones caused by their lower activity. The completeness of initiator incorporation in PPOx provides control of the number-average molecular weight as well as a possibility of polymer functionalization and synthesis of block-copolymers.

This work was carried out as a part of the Project ‘Contemporary Problems of Chemistry and Physical Chemistry of Macromolecules’ (State Assignment no. AAAA-A21-121011990022-4). The NMR measurements were carried out at the Center for Magnetic Tomography and Spectroscopy, Department of Fundamental Medicine of M. V. Lomonosov Moscow State University. The thermal analysis was performed using the equipment purchased in the scope of the M. V. Lomonosov Moscow State University Program for Development.

Online Supplementary Materials

Supplementary data associated with this article can be found in the online version at doi: 10.71267/mencom.7725.

References

1 M. A. Macchione, D. Aristizabal Bedoya, F. N. Figueroa and M. C. Strumia, in *Advances and Challenges in Pharmaceutical Technology*, Elsevier, 2021, pp. 45–73; https://doi.org/10.1016/B978-0-12-820043-8.00005-0.
2 M. A. Khavpachev, E. S. Trofimchuk, N. I. Nikonorova, E. S. Garina, M. A. Moskvina, A. V. Efimov, V. A. Demina, A. V. Bakirov, N. G. Sedush, V. V. Potseleev, T. A. Cherdyntseva and S. N. Chvalun, *Macromol. Mater. Eng.*, 2020, **305**, 2000163; https://doi.org/10.1002/mame.202000163.
3 S. P. Nischwitz, D. Popp, D. Shubitidze, H. Luze, R. Zrim, K. Klemm, M. Rapp, H. L. Haller, M. Feisst and L.-P. Kamolz, *Int. Wound J.*, 2022, **19**, 1180; https://doi.org/10.1111/iwj.13713.
4 P. A. Povernov, L. S. Shibryaeva, L. R. Lusova and A. A. Popov, *Fine Chem. Technol.*, 2022, **17**, 514; https://doi.org/10.32362/2410-6593-2022-17-6-514-536.
5 C. V. Aarsen, A. Liguori, R. Mattsson, M. H. Sipponen and M. Hakkarainen, *Chem. Rev.*, 2024, **124**, 8473; https://doi.org/10.1021/acs.chemrev.4c00032.
6 Z. Tu, Y. Lu, L. Sang, Y. Zhang, Y. Li and Z. Wei, *Macromolecules*, 2023, **56**, 3149; https://doi.org/10.1021/acs.macromol.3c00003.
7 D. Hong, B. Song, H. Kim, J. Kwon, G. Khang and D. Lee, *Ther. Delivery*, 2011, **2**, 1407; https://doi.org/10.4155/tde.11.113.
8 N. P. Iakimov, E. M. Budynina, A. K. Berkovich, M. V. Serebryakova, V. B. Platonov, E. O. Fomin, A. G. Buyanovskaya, I. V. Mikheev and N. S. Melik-Nubarov, *Eur. Polym. J.*, 2024, **220**, 113410; https://doi.org/10.1016/j.eurpolymj.2024.113410.
9 O. Dechy-Cabaret, B. Martin-Vaca and D. Bourissou, *Chem. Rev.*, 2004, **104**, 6147; https://doi.org/10.1021/cr040002s.
10 Y. Wu, K. Chen, J. Wang, M. Chen, W. Dai and R. Liu, *J. Am. Chem. Soc.*, 2024, **146**, 24189; https://doi.org/10.1021/jacs.4c05382.
11 N. Hadjichristidis, H. Iatrou, M. Pitsikalis and G. Sakellariou, *Chem. Rev.*, 2009, **109**, 5528; https://doi.org/10.1021/cr900049t.
12 E. O. Fomin, E. A. Iakimova, N. P. Iakimov, I. D. Grozdova and N. S. Melik-Nubarov, *Polym. Sci., Ser. B*, 2024, **66**, 544; https://doi.org/10.1134/S1560090424601365.
13 H. Danafar, S. Davaran, K. Rostamizadeh, H. Valizadeh and M. Hamidi, *Adv. Pharm. Bull.*, 2014, **4**, 501; https://doi.org/10.5681/apb.2014.074.
14 N. P. Iakimov, A. V. Romanyuk, I. D. Grozdova, E. A. Dets, N. V. Alov, P. Yu. Sharanov, S. V. Maksimov, S. V. Savilov, S. S. Abramchuk, A. L. Ksenofontov, E. A. Eremina and N. S. Melik-Nubarov, *Soft Matter*, 2021, **17**, 2711; https://doi.org/10.1039/D0SM02259D.
15 J. Shi, Z. Liu, N. Zhao, S. Liu and Z. Li, *Macromolecules*, 2022, **55**, 2844; https://doi.org/10.1021/acs.macromol.1c02654.
16 X. Tao, B. Zheng, T. Bai, M.-H. Li and J. Ling, *Macromolecules*, 2018, **51**, 4494; https://doi.org/10.1021/acs.macromol.8b00259.
17 M. Päch, D. Zehm, M. Lange, I. Dambowsky, J. Weiss and A. Laschewsky, *J. Am. Chem. Soc.*, 2010, **132**, 8757; https://doi.org/10.1021/ja102096u.
18 S. Thongkham, J. Monot, B. Martin-Vaca and D. Bourissou, *Macromolecules*, 2019, **52**, 8103; https://doi.org/10.1021/acs.macromol.9b01511.
19 H. Chen, M. He, J. Pei and B. Liu, *Anal. Chem.*, 2002, **74**, 6252; https://doi.org/10.1021/ac020528h.
20 S. E. Felder, M. J. Redding, A. Noel, S. M. Grayson and K. L. Wooley, *Macromolecules*, 2018, **51**, 1787; https://doi.org/10.1021/acs.macromol.7b01785.
21 G. B. Hatch and H. Adkins, *J. Am. Chem. Soc.*, 1937, **59**, 1694; https://doi.org/10.1021/ja01288a038.
22 R. Abdul-Karim, A. Hameed and M. I. Malik, *RSC Adv.*, 2017, **7**, 11786; https://doi.org/10.1039/C7RA01113J.
23 A. Kowalski, A. Duda and S. Penczek, *Macromolecules*, 2000, **33**, 7359; https://doi.org/10.1021/ma000125o.
24 H. R. Kricheldorf and A. Stricker, *Macromol. Chem. Phys.*, 2000, **201**, 2557; https://doi.org/10.1002/1521-3935(20001101)201:17<2557::AID-MACP2557>3.0.CO;2-F.

Received: 14th January 2025; Com. 25/7725